JOURNAL OF CATALYSIS **147**, 279–293 (1994)

Transient Kinetic Study of the Reaction of C_2H_4 and C_2H_6 with the Lattice and Adsorbed Oxygen Species of Li^+-Doped TiO_2 Catalysts

D. Papageorgiou, A. M. Efstathiou, and X. E. Verykios

Institute of Chemical Engineering and High Temperature Chemical Processes, Department of Chemical Engineering, University of Patras, GR-26500, Patras, Greece

Received September 20, 1993; revised January 14, 1994

A transient kinetic study of the reactions of C_2H_4 and C_2H_6 with lattice oxygen, O^{2-} (in the absence of gaseous oxygen), and "adsorbed" oxygen (in the presence of gaseous oxygen) species over undoped and Li^+-doped TiO_2 OCM catalysts was performed. The results obtained indicate that lattice oxygen is more reactive towards C_2H_6 than C_2H_4 to form mainly CO_2, whereas "adsorbed" oxygen exhibits higher reactivity towards C_2H_4. Incorporation of Li^+ cations into the lattice of TiO_2 affects significantly the reactivity of lattice oxygen towards C_2H_6 and that of "adsorbed" oxygen species towards both hydrocarbons. The interaction of C_2H_6 and C_2H_4 with the lattice oxygen of the catalysts results in the accumulation of carbonaceous species of different amounts and compositions under the same experimental conditions. Oxidation of these carbonaceous species to CO_2 follows the same mechanism with at least two steps controlling the overall process. The activation energy of these steps is larger in the case of carbonaceous species derived from C_2H_4 than in the case of those derived from C_2H_6.

INTRODUCTION

The oxidative coupling of methane (OCM) to ethane and ethylene has become a subject of intense research worldwide. From the fundamental point of view, the challenge is due to the high molecular stability of methane, which makes it difficult to activate the carbon–hydrogen bonds in a selective manner. From the practical point of view, methane, which is found in abundance (1), could function as an alternative source of hydrocarbons and oxygenates, in view of predicted shortages in the supply of conventional oil. A large number of oxide systems have been tested so far, and review papers which summarize the results obtained have appeared in the literature (1–6).

Most of the studies on the OCM reaction are mainly devoted to the activity, C_2-hydrocarbons and oxygenates selectivity of different materials, with the main goal being to achieve yields of practical interest. Relatively little work has been done towards the elucidation of the elementary steps of the carbon and oxygen reaction pathways to form the desired as well as the undesired CO_x ($x = 1, 2$) products. Quantification of surface reaction intermediate species which participate in the reaction network, and rate constants of individual reaction steps, should remain an ultimate goal in order to understand the mechanistic aspects which control the reaction pathways (7, 8). Having this information for a given catalytic system, it is then more appropriate to reason in which direction the catalyst composition might be altered in order to improve its catalytic performance.

Steady-state tracing techniques (7), which allow the *in situ* measurement of surface intermediate species and their reactivities, have recently found application in the investigation of the mechanism of OCM reaction over Li/MgO (9), La_2O_3 (10), Sm_2O_3 (11, 12), and Li^+-doped TiO_2 (13) catalysts. For all these catalyst formulations studied, it was found that the coverage of reversibly adsorbed methane is practically zero. However, there is a large reservoir of oxygen species (surface/subsurface) which participate in the formation of CO and CO_2. On the other hand, the amount of active carbon which leads to CO, CO_2, and C_2H_6 is small. It is also important to obtain a quantitative knowledge of the reactivity of C_2-hydrocarbons or oxygenates with the catalyst surface in order to better understand the selectivity aspects of the OCM reaction. Ekstrom and Lapszewicz (14), using ^{13}C-labeled ethane and ethylene, have shown that a considerable amount of CO_2 is derived from these molecules over the Li/MgO system.

We have recently reported on the transient kinetics of the reaction of CH_4 and C_2H_6 with the lattice oxygen of Li^+-doped TiO_2 catalyst using various kinds of transient experiments (15). The results obtained indicated that (a) the lattice oxygen of Li^+-doped TiO_2 catalyst, used for the oxidative coupling of methane reaction (16–18), must be considered as a total oxidation site following reaction of CH_4/He and C_2H_6/He, (b) large amounts of carbonaceous species accumulate on the catalyst surface following reaction of C_2H_6/He, a result opposite to that found for CH_4/He reaction, and (c) transient isothermal oxidation of car-

0021-9517/94 $6.00

bonaceous species formed by C_2H_6/He reaction, leading to CO_2, can be interpreted by a kinetic model based on a sequence of stepwise dehydrogenation elementary steps. Initial reaction rates of lattice oxygen with CH_4 and C_2H_6 to form CO_2, as well as the corresponding activation energies, have also been determined. Steady-state tracing in OCM reaction (13) and other transient experiments reported earlier (15) performed over the present Li^+-doped TiO_2 catalyst suggest that it is difficult from these experiments to determine the rate-limiting step(s) of the carbon pathway of CO_2 formation, under OCM reaction conditions, mainly due to the combustion reactions of C_2-hydrocarbons on the catalyst surface.

In the present work , results of the transient kinetics of C_2H_4 reaction with the lattice oxygen of Li^+-doped TiO_2 catalyst, and of the transient oxidation kinetics of carbonaceous species formed after reaction, are reported. These results are compared to those already reported for the CH_4 and C_2H_6 reactions with the lattice oxygen of the same catalyst (15). In addition, the reactivity of C_2H_4 and C_2H_6 (specific reaction rates, activation energies) towards "adsorbed" oxygen species (in the presence of gaseous oxygen in the feed stream) is reported, and a comparison is made with the corresponding reactivity with respect to lattice oxygen alone (in the absence of gaseous oxygen in the feed stream). It is shown that lattice as well as "adsorbed" oxygen species must be considered as likely participants in the combustion of C_2-hydrocarbons over Li^+-doped TiO_2 catalyst under OCM reaction conditions. However, the rate of oxidation of C_2-hydrocarbons as compared to the net rate of their formation seems to be rather small. The present results are used to discuss possible rate-limiting steps of the reaction pathway from CH_4 to CO_2. The effects of Li^+-dopant on the aforementioned kinetic parameters are established by performing similar transient kinetic studies over the undoped TiO_2 catalyst.

EXPERIMENTAL

a. Preparation and Characterization of Li^+-Doped TiO_2 Catalyst

The lithium-doped TiO_2 catalyst was prepared by the high-temperature diffusion method. Lithium nitrate was used as a precursor of the doping Li^+ cation in an appropriate amount so as to yield 2 wt.% lithium concentration (based on $Li_2O/(Li_2O + TiO_2)$). Further details of the preparation procedure applied have been reported previously (15, 16).

The BET surface areas of the undoped and 2 wt.% Li_2O-doped TiO_2 catalysts were found to be ca. 0.2 m^2/g. Other characterization measurements performed on the present catalysts, such as electrical conductivity measurements, surface acidity and basicity determination, XRD, and XPS, have been reported elsewhere (16).

b. Catalyst Treatment

Before any transient experiments were made, the catalyst sample (1 g) was treated with pure oxygen at 800°C for 2 h. Between successive transient runs with various feed mixtures, the catalyst sample was treated with a 10% O_2/He mixture at 800°C for 30 min in order to establish approximately a similar initial surface state.

c. Flow-System for Transient Studies

An appropriate flow system that allows the application of transient methods (abrupt switches in the feed gas composition) was employed in the present investigation. This system has been described in detail elsewhere (15). Analysis of the gases during transients is done by on-line mass spectrometer (VG Quadrupoles, Sensorlab 200D) equipped with a fast response inlet capillary system. The desired gas mixtures are made up in a separate gas mixing apparatus. Calibration of the mass spectrometer is performed based on a prepared mixture of a known composition. The output signal from the mass spectrometer detector is then converted to mole fraction versus time by appropriate software. Methane, ethylene, ethane, and carbon dioxide were recorded at the mass numbers (*m/e*) 15, 26, 30, and 44, respectively. The cracking coefficients of ethylene and ethane due to the $m/e = 15$, ratios of 15/26 and 15/30, respectively, have been measured and used when necessary to calculate the concentration of methane in a mixture of C_2H_4/CH_4 and C_2H_6/CH_4, respectively. All gases were used at the flow rate of 30 mL/min (ambient). The reactor used in this study has been described previously (15).

RESULTS

a. Li^+-Doped TiO_2 Catalyst

*a.*1. *Reactivity of C_2H_4 with the lattice oxygen (C_2H_4/He reaction).* Figure 1 shows the transient response of gas-phase CO_2 at 845°C, following the switch He → 10% C_2H_4/He(*t*), where *t* designates the real time of the experiment, over 2% Li_2O/TiO_2 catalyst. As the C_2H_4/He mixture starts to flow over the catalyst, an initial transient (spike) of the rate of production of CO_2 is obtained. It is found that this initial rate increases with temperature. Following the initial transient response, there is a rapid (within 30 s) decrease of CO_2 production, which further decreases slowly during the remaining period of the experiment. It is noted here that neither CO nor C_2H_6 was found to be formed during the transient shown in Fig. 1. Only H_2O was measured in addition to CO_2. Similar CO_2 transient responses have also been obtained at temperatures

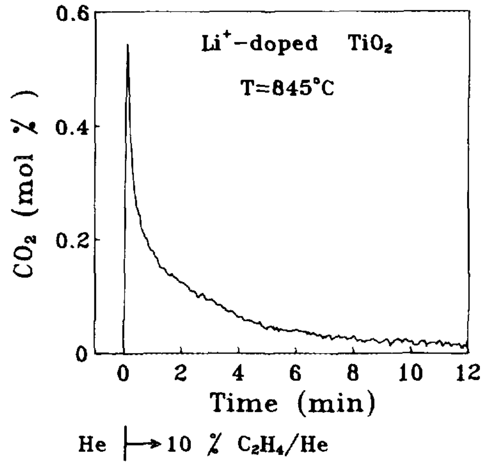

FIG. 1. Transient response of CO_2 obtained according to the delivery sequence He → 10% C_2H_4/He (845°C, *t*) over 2 wt.% Li_2O-doped TiO_2 catalyst.

in the range 740–830°C. Integration of the transient shown in Fig. 1 provides the amount of CO_2 produced (up to 10 min on stream), and this is reported in Table 1 as a function of reaction temperature. There is a progressive decrease of the amount of CO_2 produced with increasing reaction temperature. An equivalent amount of lattice oxygen species (monolayers) removed by the reaction as CO_2 can also be calculated, and this is also reported in Table 1. A monolayer of equivalent oxygen species is defined as the amount of oxygen (μmol/g) present on the catalyst surface and is calculated based on the BET surface area, the lattice parameters, and the number of surface oxygen atoms/unit cell of rutile TiO_2. The initial rate (spike) of CO_2 production shown in Fig. 1 and other initial rates obtained at lower temperatures were used to calculate the activation energy of the reaction of C_2H_4 with the lattice oxygen. This is found to be 15 kcal mol^{-1}.

a.2. Transient isothermal oxidation experiments. During reaction of C_2H_4 with the lattice oxygen of Li^+-doped TiO_2 (Fig. 1), carbonaceous species accumulate on the surface. Transient isothermal oxidation experiments of these carbonaceous species have been performed to measure their amount as a function of reaction temperature. The results obtained are shown in Fig. 2. After reaction with 10% C_2H_4/He mixture for 10 min at a given temperature, the feed is changed to He for 3 min in order to purge the reactor from the gas-phase reactant (C_2H_4), followed by a switch to a 10% O_2/He mixture. During the latter switch CO_2 is produced and its response is shown in Fig. 2. It is noted that only a very small amount of CO (less than 100 ppm) has been measured during these oxygen titration experiments. It is found that the carbonaceous species are very reactive towards oxygen, and the reaction is complete after 60 s (all carbonaceous species have essentially been reacted with oxygen). In addition, a shoulder appears in the CO_2 response curve after about 40 s of reaction time which diminishes with increasing reaction temperature. Note also that there is only a small shift in the time of appearance of the CO_2 peak maximum, t_m, with reaction temperature in the range 800–845°C. The amount of carbonaceous species accumulated on the surface (μmol/g) can be calculated based on the area under the transients shown in Fig. 2, and this is given in Table 1 as a function of reaction temperature. There is a decrease in the amount of carbonaceous species formed on the surface with increasing reaction temperature, following the same behaviour as the amount of lattice oxygen removed by C_2H_4/He reaction (Table 1).

TABLE 1

Amount of CO_2 Produced during the Sequence He → 10% C_2H_4/He (*T*, 10 min) → He (*T*, 3 min) → 10% O_2/He (*T*, *t*) over 2 wt.% Li_2O-Doped TiO_2 Catalyst

	CO_2(μmol/g)	
T(°C)	C_2H_4/He	O_2/He
780	7.8 (1.3)[a]	60.0
800	6.6 (1.1)	54.8
830	5.2 (0.9)	40.7
845	3.8 (0.6)	31.8

[a] The number in parentheses corresponds to monolayers of lattice oxygen participating in the reaction of CO_2 formation.

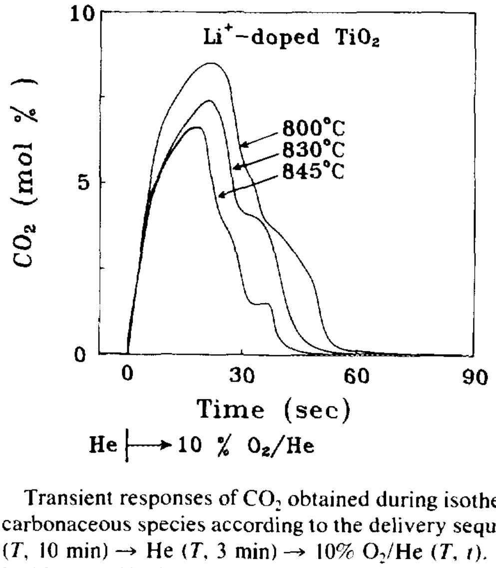

FIG. 2. Transient responses of CO_2 obtained during isothermal oxidation of carbonaceous species according to the delivery sequence 10% C_2H_4/He (*T*, 10 min) → He (*T*, 3 min) → 10% O_2/He (*T*, *t*), *T* = 800, 830, and 845°C; 2 wt.% Li_2O-doped TiO_2 catalyst.

Transient isothermal oxidation experiments of carbonaceous species formed after reaction of C_2H_4 with the lattice oxygen of the catalyst at 845°C were also conducted at different temperatures. The experimental procedure was as follows: After reaction of the catalyst with a 10% C_2H_4/He mixture at 845°C for 10 min, the feed was changed to He and at the same time the reactor was cooled to a certain temperature, followed by a switch to a 10% O_2/He mixture. The reaction product transients obtained from the latter oxygen titration step were followed with time with on-line mass spectrometry. Only CO_2 and H_2O were measured, and the CO_2 transients are shown in Fig. 3 for oxygen titration temperatures of 570, 600, and 640°C.

It is observed in Fig. 3 that at 640°C, upon switching to the O_2/He mixture, a rapid increase in the rate of production of CO_2 is obtained, which decreases with decreasing reaction temperature (i.e., 600°C, Fig. 3). However, at somewhat lower reaction temperatures (570°C), the initial rate of CO_2 production becomes very small, and the CO_2 peak maximum of the transient response shifts to a higher reaction time, t_m, with respect to that obtained at higher reaction temperatures (Fig. 3, 600°C). It is noted that an increase in the temperature of the catalyst bed by 2–3°C was observed upon switching to the O_2/He mixture at 700°C; this temperature change lasted for only 15 s. The reaction times in oxygen flow for the appearance of the CO_2 peak maximum (t_m) are found to be 200, 65, 30, and 15 s for titration temperatures of 570, 600, 640, and 700°C, respectively. In a later section it is shown how these experimental data of t_m vs reaction temperature (T) could be used to estimate the activation energy of the oxidation of these carbonaceous species to CO_2. It is noted that the total amount of carbonaceous species removed by oxygen in the experiments of Fig. 3 is approximately the same (40 μmol/g) at all reaction temperatures. The latter result is opposite to that reported in the case of C_2H_6/He reaction (15).

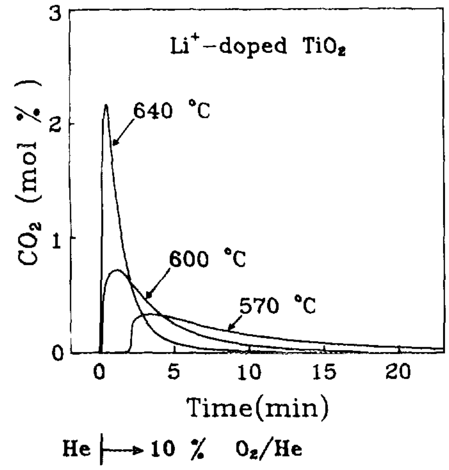

FIG. 3. Transient responses of CO_2 obtained during isothermal oxidation of carbonaceous species according to the delivery sequence 10% C_2H_4/He (845°C, 10 min) → He cool to T → 10% O_2/He (T, t). T = 570, 600, and 640°C; 2 wt.% Li_2O-doped TiO_2 catalyst.

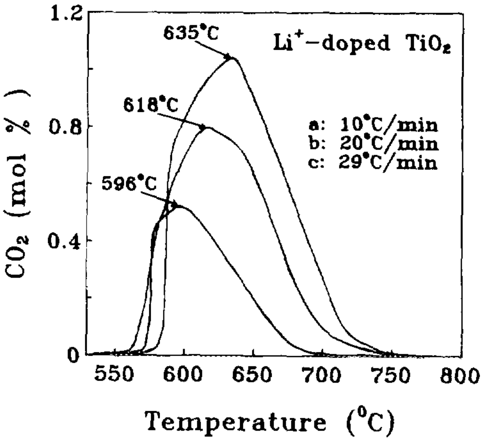

FIG. 4. Temperature-programmed oxidation (TPO) of carbonaceous species formed by C_2H_4 reaction with the lattice oxygen of 2 wt.% Li_2O-doped TiO_2 catalyst. Delivery sequence: 10% C_2H_4/He (845°C, 10 min) → He, cool to 400°C → 10% O_2/He, TPO. Results are shown for heating rates of 10, 20, and 29°C/min.

a.3. Temperature-programmed oxidation experiments. Figure 4 shows CO_2 responses obtained during temperature-programmed oxidation (TPO) experiments, with a varying heating rate, β, in the range 10–40°C/min, of carbonaceous species formed after C_2H_4/He reaction at 845°C over Li^+-doped TiO_2 catalyst. After the catalyst was treated with 10% C_2H_4/He mixture at 845°C for 10 min, the feed was changed to He while, at the same time, the reactor was cooled to 400°C. Then, the feed was changed to 10% O_2/He mixture with a simultaneous linear increase of the temperature to 850°C. As is clearly shown in Fig. 4, there is a shift in the peak maximum temperature (T_M) of the CO_2 response obtained with varying heating rate, β. This feature is used to calculate the activation energy of oxidation of carbonaceous species formed by reaction of C_2H_4 with the lattice oxygen of the catalyst, which is compared to the activation energy value obtained based on the isothermal transient oxidation experiments shown in Fig. 3. These calculation procedures of the activation energy are described below.

a.4. Kinetic model for the oxidation of carbonaceous species. In a recent publication from this laboratory (15), a kinetic model of the oxidation of carbonaceous species formed upon reaction of C_2H_6 with the lattice oxygen of the Li^+-doped TiO_2 catalyst was presented. Shifts in the time of appearance of CO_2 peak maxima were used to obtain kinetic parameters (i.e., activation energy and number of rate-determining steps). The results presented in Fig. 3 show a similar behaviour as that mentioned above. In the present case carbonaceous species are formed upon reaction of C_2H_4 with the lattice oxygen of the catalyst. It is proposed that CH_x and/or CH_xO (x = 0–2) species might be considered as precursor intermediate species which are formed and accumulate on the catalyst surface. Some of these species react further with lattice oxygen to form CO_2 (Fig. 1). It is important to state here that no molecularly adsorbed C_2H_4, or an intermediate species which could decompose to C_2H_4, is formed following reaction of C_2H_4/He with lattice oxygen. This statement is based on the fact that no C_2H_4 was detected during He purge, following C_2H_4/He reaction in the temperature range 780–845°C (Fig. 1).

The elementary steps which have been proposed (15) to comprise the mechanism of oxidation of CH_x and/or CH_xO species in the presence of gas-phase oxygen to form CO_2 (Fig. 3) are

$$O_2(g) + (2e^- \mid \square_S) \leftrightarrows (O^{2-} \mid \square_S) + O(a) \quad [1]$$

$$CH_x(a) + O(s) \rightarrow CH_{x-1}(a) + OH(s) \quad [2]$$

$$CH_{x-1}(a) + O(s) \rightarrow CH_{x-2}(a) + OH(s) \quad [3]$$

$$C(a) + O(s) \rightarrow CO(a) + (s) \quad [4]$$

$$CO(a) + O(s) \rightarrow CO_2(g) + (s) \quad [5]$$

$$2OH(s) \rightarrow H_2O + O(s) + \square_S, \quad [6]$$

where Steps [2] and [3] apply for x = 2 ($-CH_2$ and $-CH$ species). Here, $\square_S$ is an oxygen vacancy, O^{2-} is a lattice oxygen species, O(a) is an "adsorbed" atomic oxygen species, $CH_x(a)$, x = 1–2, is an adsorbed hydrocarbon species, O(s) is an atomic oxygen species (lattice or "adsorbed" oxygen), OH(s) is a hydroxyl species associated with the O(s) species, and (s) is a site. Here, "adsorbed" oxygen species are considered to be those which are formed according to reaction Step [1] and may include O^-, O_2^-, and O^{2-} species in accordance with what has been reported in the literature (5, 6).

For the case of a $-CH_xO$ species, steps similar to [2], [3], and [5] can be written, whereas Step [4] may be absent from the above-described sequence of steps. If it is assumed that (a) the rate-determining steps (if more than one step) of the above-described sequence of Steps [2]–[5] have the same rate constant k, (b) Step [1] is not rate determining, and (c) the concentration of O(s) species remains practically constant during the transient oxidation experiments, then the following expression for t_m can be obtained (15):

$$t_m = \frac{\alpha - 1}{k_o \exp(-E/RT)[O_S]}. \quad [7]$$

Here, t_m is the time of appearance of the peak maximum in the CO_2 response during transient isothermal oxidation, α is the number of elementary steps with the same rate constant, k, which control the rate of formation of CO_2, and $[O_S]$ is the concentration of O(s) species. The rate constant k is given by the Arrhenius relationship $k = k_O \exp(-E/RT)$, where E is the activation energy of the oxidation of $-CH_x$ and/or $-CH_xO$ species. Equation [7] can be rearranged to give

$$\ln(t_m) = \ln\left(\frac{\alpha - 1}{k_O[O_S]}\right) + (E/R)\left(\frac{1}{T}\right). \quad [8]$$

The results of Fig. 3 and Eq. [8] are used to obtain the activation energy of oxidation of the carbonaceous species formed by reaction of C_2H_4 with the lattice oxygen of the Li^+-doped TiO_2 catalyst. This is illustrated in Fig. 5a, from which an activation energy of 34 kcal mol^{-1} is estimated. The good fit of the data to the model is noted.

The experimental results of Fig. 4 can also be used to test the kinetic scheme described above. The analysis is based on a similar work of Bianchi and Gass (19) for the sequential hydrogenation of a carbon-containing species, CH_x, during a temperature-programmed hydrogenation

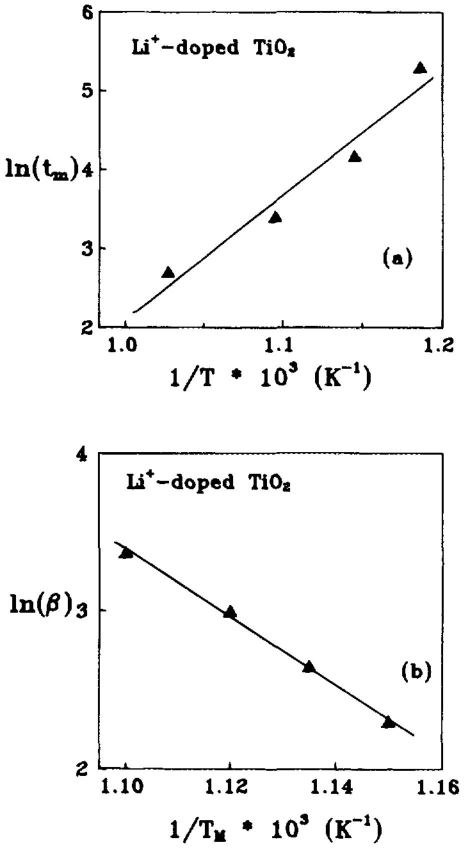

FIG. 5. (a) Application of Eq. [8] of the kinetic model used for the isothermal oxidation of carbonaceous species formed upon reaction of C_2H_4 with the lattice oxygen of 2 wt.% Li_2O-doped TiO_2 catalyst. (b) Application of Eq. [11] of the kinetic model used for the temperature-programmed oxidation of carbonaceous species formed upon reaction of C_2H_4 with the lattice oxygen of 2 wt.% Li_2O-doped TiO_2 catalyst.

process. Their analysis applies equally well to the present sequential dehydrogenation/oxidation mechanism of Steps [2]–[5] under temperature-programmed oxidation conditions. In the present work, the approximation that oxygen chemisorption (Step [1]) follows the Langmuir model is also applied, as in the case of H_2 chemisorption (19), and, in addition, that the concentration of "adsorbed" oxygen species, $[O_S]$, is approximated by

$$[O_S] = \sqrt{KP_{O_2}} \cdot [O_S]_O, \qquad [9]$$

where $\sqrt{KP_{O_2}} < 1$ (valid at high temperatures), and $[O_S]_O$ is the concentration of "adsorbed" oxygen species at saturation.

The analysis presented by Bianchi and Gass (19) reveals that with or without considering rate-limiting steps in the above-given sequence of Steps [2]–[5], the same relationship between the peak maximum temperature, T_M, and the activation energy, E, of oxidation of CH_x species is obtained, given by

$$E = R\,T_M \ln\left(\frac{k_O[O_S]}{\beta}\right). \qquad [10]$$

Equation [10] can be rearranged to give

$$\ln\beta = \ln(k_O[O_S]) - \left(\frac{E}{R}\right)\left(\frac{1}{T_M}\right). \qquad [11]$$

By varying the heating rate, β, T_M is expected to vary, and the activation energy, E, can be estimated using Eq. [11]. Figure 5b shows the application of Eq. [11] using the experimental results presented in Fig. 4. An activation energy of 38 kcal mol^{-1} is calculated, a value which is in good agreement with that obtained from the results of Fig. 5a. Thus, the mechanistic scheme of the sequential dehydrogenation/oxidation of $-CH_x$ and/or $-CH_xO$ species has been probed using two independent kinds of experiments which produced a similar activation energy for the oxidation of the aforementioned carbonaceous species produced upon interaction of C_2H_4 with the lattice oxygen of Li^+-doped TiO_2 catalyst.

b. TiO_2 Catalyst

b.1. Reactivity of C_2H_4 with the lattice oxygen (C_2H_4/He reaction). Figure 6 shows transient responses of gas-phase CO_2 and CH_4 at 800 and 845°C obtained over undoped TiO_2, following the switch He → 10% C_2H_4/He (t). In the present case, in addition to CO_2 methane is also produced, a result opposite to that obtained with the Li^+-doped TiO_2 catalyst (Fig. 1). In the range 800–845°C, there is a decrease in the amount of CO_2 produced and an increase in the corresponding amount of CH_4 with increasing reaction temperature. The quantities of CO_2 and CH_4 produced at different temperatures are given in Table 2. Worth noting is the appearance of two peaks in the response of CH_4 and only one peak in the response of CO_2 at 845°C. The initial rates of reaction of C_2H_4 with the lattice oxygen of TiO_2 to form CO_2 and CH_4 (Fig. 6) are used to calculate activation energies, which are found to be 14 and 65 kcal mol^{-1}, respectively.

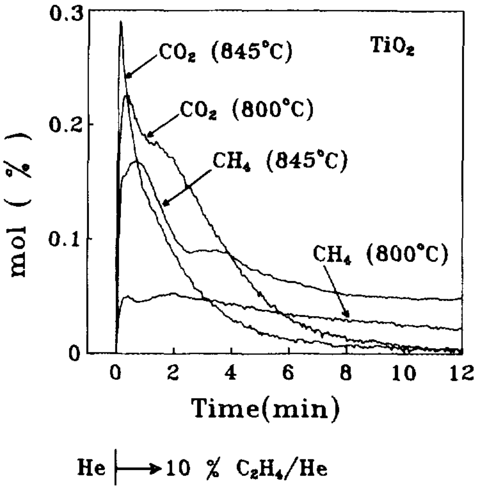

FIG. 6. Transient responses of CO_2 and CH_4 obtained according to the delivery sequence He → 10% C_2H_4/He (T, t). T = 800 and 845°C; undoped TiO_2 catalyst.

Transient isothermal oxidation experiments, similar to those described in Fig. 2, have been performed to measure the amount of carbonaceous species accumulated on the surface of TiO_2 following reaction with C_2H_4/He for 10 min. The amount of carbonaceous species removed by this oxygen treatment as a function of reaction temperature is given in Table 2. There is an increase of carbonaceous species accumulated on the surface with reaction temperature, a result opposite to that found for the amount of lattice oxygen participating in the reaction of CO_2 formation (Table 2).

TABLE 2

Amounts of CO_2 and CH_4 Produced during the Sequence He → 10% C_2H_4/He (T, 10 min) →He (T, 3 min) → 10% O_2/He (T, t) over TiO_2 Catalyst

	C_2H_4/He		O_2/He
T(°C)	CO_2(μmol/g)	CH_4(μmol/g)	CO_2(μmol/g)
800	9.0 (1.5)[a]	4.8	8.5
820	6.3 (1.1)	5.5	10.0
845	5.6 (0.9)	10.3	15.0

[a] The number in parentheses corresponds to monolayers of lattice oxygen participating in the reaction of CO_2 formation.

b.2. Transient isothermal oxidation experiments following reaction with C_2H_4/He or C_2H_6/He. In order to check whether the oxidation of carbonaceous species formed after reaction of C_2H_4 or C_2H_6 with the lattice oxygen of undoped TiO_2 follows the same mechanistic scheme as that previously presented for the case of C_2H_4/He reaction and C_2H_6/He reaction (15) over Li^+-doped TiO_2 catalyst, similar experiments have been conducted over the undoped TiO_2 catalyst. After exposing the catalyst to 10% C_2H_4/He or 10% C_2H_6/He mixtures at 845°C for 10 min, the feed is changed to He, and simultaneously the reactor is cooled to a certain temperature, followed by a switch to a 10% O_2/He mixture. The CO_2 transient responses obtained at various oxygen titration temperatures are given in Figs. 7 and 8 for the case of C_2H_4/He and C_2H_6/He reactions, respectively. In the case of C_2H_4/He reaction, Fig. 7 clearly shows that there is a shift in the time of appearance of the peak maximum of the CO_2 response, as observed in Fig. 3 with Li^+-doped TiO_2 and predicted by the kinetic model presented (see Eq. [7]). The amount of carbonaceous species removed at each temperature is found to be practically the same as that formed during the reaction of C_2H_4 with the lattice oxygen of TiO_2 at 845°C. However, in the case of C_2H_6/He reaction (Fig. 8) the amount of carbonaceous species removed by oxygen titration decreases with increasing temperature (Table 3). This behaviour is similar to that reported earlier over the Li^+-doped TiO_2 catalyst (15). At the lowest temperature studied (700°C, in Fig. 8), there is an initial sharp increase (spike) in the rate of production of CO_2 as the O_2/He mixture starts to flow over the catalyst. This is followed by a quick achievement of a practically constant value of the rate of production of CO_2, which lasts for about 5 min. Then, the rate of reaction increases and goes through a second maximum. On the other hand, at higher temperatures (820°C, in Fig. 8) the rate of production of CO_2 during the first 5 min of reaction is much smaller than that observed at 700°C, and only a single, relatively narrow, CO_2 peak is formed. The peak maximum of this CO_2 peak is found to shift towards higher times of reaction in oxygen flow with decreasing reaction temperature. This behaviour is illustrated in Table 3. Equation [8] is used to analyze the observed shifts in the time of appearance of peak maximum of CO_2 response in Figs. 7 and 8. Activation energies of 23 and 8 kcal mol^{-1} are estimated for the oxidation of carbonaceous species formed following reaction of C_2H_4 and C_2H_6 with the lattice oxygen of TiO_2, respectively.

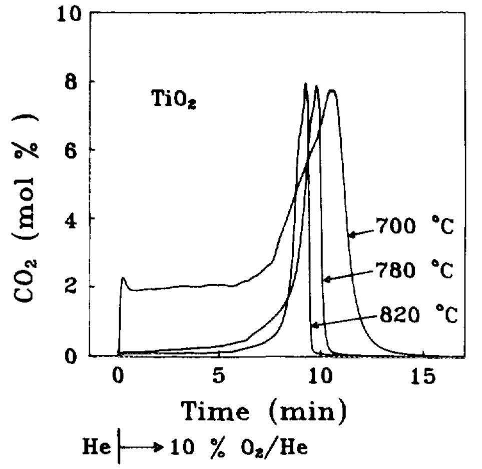

FIG. 8. Transient responses of CO_2 obtained during isothermal oxidation of carbonaceous species according to the delivery sequence 10% C_2H_6/He (845°C, 10 min) → He, cool to T → 10% O_2/He (T, t). T = 700, 780, and 820°C; undoped TiO_2 catalyst.

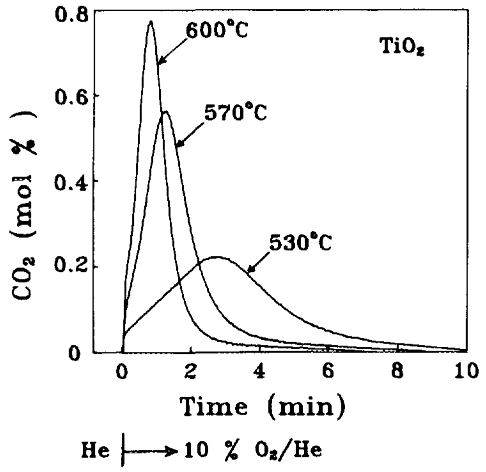

FIG. 7. Transient responses of CO_2 obtained during isothermal oxidation of carbonaceous species according to the delivery sequence 10% C_2H_4/He (845°C, 10 min) → He, cool to T → 10% O_2/He (T, t). T = 530, 570, and 600°C; undoped TiO_2 catalyst.

TABLE 3

Amount of Carbon Species Removed by Oxygen, the Former Species Produced by C_2H_6/He or C_2H_4/He Reaction with TiO_2 at 845°C

C_2H_6/He			C_2H_4/He^a		
carbon species			carbon species		
T(°C)	(μmol/g)	t_{max} (s)	T(°C)	(μmol/g)	t_{max} (s)
700	473.0	634	530	15.8	155
740	235.6	585	570	16.3	74
780	147.0	555	600	16.5	48
820	87.0	520	700	16.7	12

Note. Delivery sequence: 10% C_2H_6/He or 10% C_2H_4/He (845°C, 10 min) → He, cool to T → 10% O_2/He (T, t). Also shown is the time of appearance, t_{max}, of the CO_2 peak maximum during oxygen treatment.

[a] The amount of carbon species removed by oxygen is found to be independent of temperature during oxygen titration.

TABLE 4

Activation Energy of Oxidation of Carbon Species to Form CO_2, the Former Produced by Reaction of C_2H_4 and C_2H_6 with the Lattice Oxygen of TiO_2 and 2 wt.% Li_2O-Doped TiO_2 Catalysts

Reactant molecule	E (kcal/mol)	
	TiO_2	2 wt.% Li_2O-doped TiO_2
C_2H_4	23	35
C_2H_6	8	15[a]

[a] From Ref. (15).

Table 4 summarizes the activation energy values of oxidation of carbonaceous species formed upon reaction of C_2H_4 or C_2H_6 over TiO_2 and Li^+-doped TiO_2 catalysts, as estimated from the transient isothermal oxidation experiments shown in Figs. 3, 7, and 8 and the kinetic model previously described. These results show that the oxidation of carbonaceous species proceeds with a lower activation energy when these species are formed over the surface of TiO_2 than over Li^+-doped TiO_2 catalyst.

b.3. Reactivity of C_2H_4 and C_2H_6 with "adsorbed" oxygen species (C_2H_4/O_2 and C_2H_6/O_2 reactions). In order to study the reactivity of "adsorbed" oxygen species towards C_2H_4 and C_2H_6, transient experiments with C_2H_4/O_2 and C_2H_6/O_2 mixtures in the range 570–700°C have been conducted. It was determined that, under the present experimental conditions, gas-phase oxidation reactions of C_2H_4 and C_2H_6 leading to CO_2 were absent below 680°C, while at 700°C gas-phase reactions contributed to only 15% of the total rate of CO_2 formation.

Figures 9a and 9b show transient responses of CO_2 formation at 670 and 700°C after switching the feed from He to C_2H_6/O_2/He or C_2H_4/O_2/He mixture, respectively, over the TiO_2 catalyst. In all experiments there is a relatively rapid increase in the rate of production of CO_2 upon switching to the reaction mixture, while within 3 min on stream a steady-state value in the rate of reaction is achieved. In the case of the C_2H_6/O_2 reaction, only CO_2 was detected, while in the case of C_2H_4/O_2 reaction, in addition to CO_2, small quantities of CH_4 were detected (Fig. 9b). Similar CO_2 transient responses have been obtained over the 2 wt.% Li^+-doped TiO_2 catalyst. However, for the latter catalyst formulation, the steady-state rate of CO_2 formation obtained with C_2H_4/O_2/He feed decreases with increasing reaction temperature in the range 570–700°C. Oxygen titration experiments of the catalyst surface following reaction with either C_2H_6/O_2/He or C_2H_4/O_2He mixtures, similar to those of Fig. 2, showed that there is only a small amount of carbonaceous species accumulated on the catalyst surface under these conditions (2 μmol/g at 700°C), in contrast to the case in which no oxygen is present in the feed stream (Fig. 1).

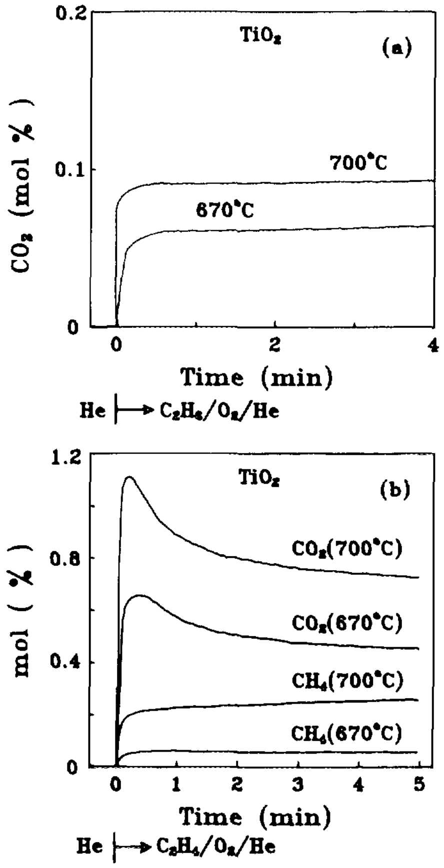

FIG. 9. (a) Transient responses of CO_2 obtained according to the delivery sequence He → 8% C_2H_6/6.6% O_2/He (*T*, *t*). (b) Transient responses of CH_4 and CO_2 according to the delivery sequence He → 8% C_2H_4/6.6% O_2/He (*T*, *t*). T = 670 and 700°C; undoped TiO_2 catalyst.

c. Rates of Reaction of C_2H_6 and C_2H_4 with Lattice and "Adsorbed" Oxygen Species.

It is very instructive to compare the reactivity of C_2H_6 and C_2H_4 with lattice and "adsorbed" oxygen species of TiO_2 and Li^+-doped TiO_2 catalysts. In the case of reaction with lattice oxygen, initial rates are used, estimated from the results of Fig. 1 and others reported earlier (15). In the case of reaction with "adsorbed" oxygen species (C_2H_6/O_2 or C_2H_4/O_2 feed mixtures) the steady-state values are used, such as those obtained from Fig. 9. Tables 5 and 6 present these results for the case of C_2H_6 and C_2H_4, respectively. In these tables, R_1 is the specific reaction rate of CO_2 formation (μmol/min m^2) from the reaction of C_2H_6 and C_2H_4 with lattice oxygen, and R_2 is the corresponding specific reaction rate with "adsorbed" oxygen species. In the case of C_2H_6, it clearly appears that the lattice oxygen of both undoped and 2 wt.% Li^+-

TABLE 5

Rates of Reaction of Lattice (R_1) and "Adsorbed" (R_2) Oxygen Species with C_2H_6 to Form CO_2 over TiO_2 and Li^+-Doped TiO_2 Catalysts

	Rate$_{CO_2}$ (μmol/min m^2)			
	TiO_2		2 wt.% Li^+-doped TiO_2	
T(°C)	R_1[a]	R_2	R_1[a]	R_2
650	—	1.9	—	1.1
670	—	3.0	—	1.4
680	234	3.5	25	1.6
700	262	5.3	35	2.1
740	433	—	—	—
780	520	—	122	—
815	615	—	170	—
820	665	—	190	—
845	—	—	282	—

[a] From Ref. (15).

TABLE 7

Activation Energies of Formation of Products of Reaction of CH_4, C_2H_4, and C_2H_6 with the Lattice Oxygen of TiO_2 and 2 wt.% Li_2O-Doped TiO_2 Catalysts

	E (kcal/mol)		
	TiO_2		2 wt.% Li_2O-doped TiO_2
	Product molecule		Product molecule
Reactant mixture	CO_2	CH_4	CO_2
5% CH_4/He	—		35[a]
10% C_2H_4/He	16.4	65	13
10% C_2H_6/He	15.5	—	28[a]
25% CH_4/5% O_2/He	32[b]		38[b]
8% C_2H_4/6.6% O_2/He	10	60	7[c]
8% C_2H_6/6.6% O_2/He	35.8	—	24.5

Note. Also given are the activation energies of formation of products of CH_4/O_2, C_2H_4/O_2, and C_2H_6/O_2 reactions.

[a] From Ref. (15).

[b] From Ref. (16).

[c] Negative apparent activation energy (see Table 6).

doped TiO_2 catalysts is much more reactive than "adsorbed" oxygen species to form CO_2. On the other hand, in the case of C_2H_4 the opposite behaviour is observed (Table 6), namely, "adsorbed" oxygen species appear to be more reactive towards C_2H_4 than lattice oxygen. Worth noting is the decrease of the specific reaction rate with increasing reaction temperature in the case of C_2H_4/O_2 reaction over Li^+-doped TiO_2 catalyst, a result not observed over TiO_2 catalyst (Table 6).

TABLE 6

Rates of Reaction of Lattice (R_1) and "Adsorbed" (R_2) Oxygen Species with C_2H_4 to Form CO_2 over TiO_2 and Li^+-Doped TiO_2 Catalysts

	Rate$_{CO_2}$ (μmol/min m^2)			
	TiO_2		2 wt.% Li^+-doped TiO_2	
T(°C)	R_1	R_2	R_1	R_2
570	—	20	—	130
600	—	25	—	110
650	—	37	—	90
670	4.9	40	5.2	85
700	6.3	70	6.4	82
800	14.0	—	12.0	—
820	16.7	—	13.8	—
830	17.4	—	14.6	—
845	18.5	—	15.3	—

Table 7 (first three rows) reports the activation energy values of the formation of the products of reaction of CH_4, C_2H_4, and C_2H_6 with the lattice oxygen of TiO_2 and 2 wt.% Li_2O-doped TiO_2 catalysts. The values reported are calculated based on the initial rates of reaction (i.e., sharp peak in Fig. 1). In Table 7 (last three rows) the activation energy values of the formation of the products of reactions of CH_4/O_2, C_2H_4/O_2, and C_2H_6/O_2 are also reported. These values are calculated based on the steady-state reaction rate results shown in Fig. 9 and those reported previously (CH_4/O_2 reaction, Ref. (16)). Note the negative apparent activation energy for the case of C_2H_4/O_2 reaction over the Li^+-doped TiO_2 catalyst (Table 7, last column). The activation energy results presented in Table 7 are discussed later with respect to possible rate-determining steps for the reaction pathway from CH_4 to CO_2 under OCM reaction conditions.

d. Effect of Catalyst Pretreatment Time in Oxygen Flow on the Transient Formation of CO_2 Following C_2H_6/O_2 Reaction

The effect of catalyst pretreatment time in oxygen flow on the transient kinetics of CO_2 formation from the interaction of C_2H_6/O_2 with the surface of Li^+-doped TiO_2 catalyst was studied as follows: The catalyst was first treated in oxygen flow at 820°C for a variable period of time, Δ*t*, between 15 and 120 min. The feed was then

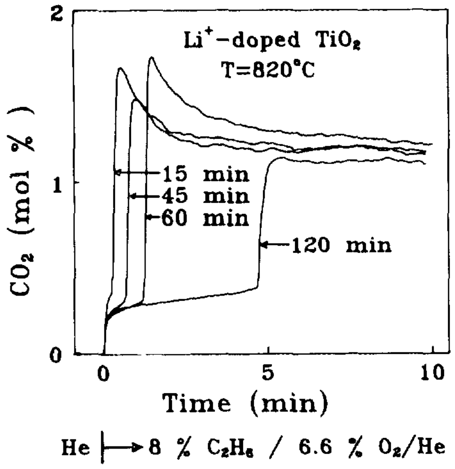

FIG. 10. Effect of catalyst pretreatment time, Δt, under O_2 flow on the transient formation of CO_2 according to the delivery sequence 10% O_2/He (820°C, Δt) → He (820°C, 10 min) → 8% C_2H_6/6.6% O_2/He (820°C, t). Δt = 15, 45, 60, and 120 min; 2 wt.% Li_2O-doped TiO_2 catalyst.

switched to He for 3 min, and then to the C_2H_6/O_2 feed mixture. Figure 10 shows the transient responses of CO_2 obtained as a function of oxygen pretreatment time, Δt, after passing C_2H_6/O_2 mixture over the catalyst. Upon switching to the reactant mixture, there is an abrupt increase in the rate of formation of CO_2. The rate increases further in a way that strongly depends on the oxygen pretreatment time. More precisely, as the time Δt increases, (a) the rate of increase of the initial reaction rate becomes smaller and (b) the second overshoot in the reaction rate observed shifts significantly to higher reaction times. However, the steady-state reaction rate obtained in all cases is practically the same. Similar experiments performed over the undoped TiO_2 catalyst revealed the absence of these oxygen pretreatment effects shown in Fig. 10.

DISCUSSION

a. Reactivity of Lattice Oxygen towards C_2H_4

*a.*1. *Effects of Li^+-dopant.* The effects of Li^+-dopant on the reactivity of lattice oxygen of TiO_2 towards C_2H_4 are clearly demonstrated in Figs. 1 and 6 and in Tables 1, 2, and 6. There are significant differences in the transient kinetics of C_2H_4 reaction with lattice oxygen to form CO_2 between undoped TiO_2 (Fig. 6) and 2 wt.% Li_2O-doped TiO_2 (Fig. 1) catalysts in the temperature range 780–820°C. For instance, at 800°C the CO_2 response obtained over TiO_2 shows a large broadening after about 1 min of reaction (shoulder at the right of first peak), and the appearance of the maximum of the first peak occurs at a t_m different than zero, in contrast to the case of reaction at 845°C (t_m = 0). These results are not observed over Li^+-doped TiO_2 catalyst. In addition, in the case of TiO_2 there is a clear production of CH_4, following reaction with C_2H_4/He, a result not seen in the case of Li^+-doped TiO_2.

To understand the effects of reaction temperature on the transient kinetics of CO_2 formation (responses shown in Figs. 1 and 6) a complete mathematical model, based on a sequence of elementary steps, including adsorption of C_2H_4 and subsequent oxidation steps to form CO_2, is required. This model must also account for the change in the concentration of surface lattice oxygen with reaction time due to consumption by reaction and to diffusion from the bulk of the solid. However, this task is beyond the scope of the present work. Instead, the kinetic model of the oxidation of carbonaceous species formed after C_2H_4 reaction with the lattice oxygen presented under Results is used here to explain the main features of the CO_2 transient responses shown in Figs. 1 and 6.

In the case of C_2H_4 reaction with the lattice oxygen of Li^+-doped TiO_2 (Fig. 1) in the temperature range 780–845°C, the observed maximum in the rate of CO_2 formation occurs at t_m = 0. During the 30 s of reaction time (which is essentially required to form the CO_2 peak) the equivalent oxygen consumption is 10% of a monolayer (see Table 1). Given the fact that some oxygen diffusion from the bulk to the surface at 845°C is expected, there is only a small decrease in the concentration of lattice oxygen species involved in the reaction during the first 30 s of time on stream. Using Eq [7] it can then be seen that t_m becomes zero only if there is one rate-limiting step in the carbon oxidation pathway to form CO_2. Therefore, the observed shift of the peak maximum of CO_2 response for the case of undoped TiO_2 (Fig. 6) may be due to the fact that more than one rate-limiting step is involved in the formation of CO_2. The shoulder then observed at 800°C may be associated with a second kind of carbonaceous species, a result consistent with the fact that more than one step controls the overall reaction process.

The quantitative results shown in Tables 1 and 2 (amount of equivalent carbon consumed during reaction, which is the sum of gas-phase CO_2 and CH_4 produced during reaction and the carbon removed by O_2 as CO_2 at the end of reaction) clearly show that the surface of the 2 wt.% Li_2O-doped TiO_2 catalyst is more active than that of the undoped TiO_2 since, for the same time on stream (10 min), the amount of C_2H_4 consumed is larger in Li^+-doped than in undoped TiO_2 catalyst. Several factors may contribute to this behaviour and these are discussed below.

XPS measurements performed on the present Li^+-doped TiO_2 catalyst indicate that Li^+-dopant cations segregate on the surface at the expense of Ti^{4+} cations (16); a ratio of Ti/O = 0.52 in the undoped TiO_2 vs 0.35 in the

Li^+-doped TiO_2 was found. These results then imply less electron charge withdrawal from the lattice oxygen species, so that their effective negative charge would be greater than that in the case of undoped TiO_2 surface. Considering the fact that hydrogen abstraction mechanism by O^{n-} species, followed by C–C bond breaking, is likely the most operative activation mechanism of C_2-hydrocarbon combustion over the present catalysts (20), the rate of hydrogen abstraction would be expected to be higher over the Li^+-doped than the undoped TiO_2 surface, and in turn the rate of C–C bond breaking and the overall consumption rate of C_2H_4. It is also relevant to say that the CH_x and/or CH_xO species formed during C_2H_4/He reaction with the catalyst surface may block active sites necessary for hydrogen abstraction and C–C bond cleavage to a greater extent in TiO_2 than in Li^+-doped TiO_2 catalyst.

Recent transient isotopic work with $^{18}O_2$ over the present catalysts revealed that the activation energy of bulk lattice oxygen diffusion over the 2 wt.% Li_2O-doped TiO_2 is smaller by 6 kcal/mol than that of the undoped TiO_2 catalyst (17). Thus, the rate of diffusion of lattice oxygen from the bulk to the surface during the transient reaction of C_2H_4 with the catalyst surface (Figs. 1 and 6), due to an oxygen concentration gradient developed via surface oxygen consumption, is expected to be higher in the case of Li^+-doped TiO_2. Considering also the kinetic model presented earlier, it is reasonable to expect higher rates of C_2H_4 consumption towards formation of carbonaceous intermediate species (CH_xO), some of which eventually lead to gaseous CO_2, over the latter catalyst. The activation energy results shown in Table 4 support the view that Li^+-dopant affects one of the oxidation steps of CH_x and/or CH_xO species which lead to CO_2.

a.2. Comparison of the reactivities of C_2H_4 and C_2H_6 with lattice oxygen. The isothermal transient reaction of C_2H_4 with the lattice oxygen species of Li^+-doped TiO_2 catalyst to form CO_2 in the range 740–845°C (Fig. 1) produced a single peak with a peak maximum at $t = 0$ and an exponential-like decay. However, the reaction of C_2H_6 with the lattice oxygen species of the same catalyst at 745°C produced three peaks during a similar experiment to that shown in Fig. 1 (15). The appearance of the first peak (overshoot at $t = 0$) is similar to that observed in Fig. 1 and is in agreement with the initially high surface concentration of lattice oxygen species. On the other hand, the appearance of the second and third peaks in the case of C_2H_6 (15), not observed in the case of C_2H_4 (Fig. 1), has been suggested to be due to the way the carbonaceous species are formed on the surface during C_2H_6/He reaction. It has been proposed that during surface lattice oxygen consumption, carbonaceous species accumulate in "island" forms on the surface. When a critical carbon and oxygen surface coverage occurs, the latter due to bulk lattice oxygen diffusion to the surface, reaction takes place whose rate is even larger than that corresponding to peak 1 (initial rate) due to the high surface concentration of carbonaceous species. A local temperature excursion from the exotherm of the combustion reaction may also contribute to this phenomenon (a temperature increase of 2–3°C in the middle of the catalyst bed was measured).

Based on the discussion above, it is logical to propose that the differences in the transient kinetics of C_2H_4 (Fig. 1) and C_2H_6 reaction (15) with lattice oxygen to form CO_2 must largely be due to differences in the kinds of carbonaceous species (CH_x and/or CH_xO) and their kinetics of dehydrogenation and oxidation to form CO_2. Evidence for the latter is given in Table 4, where large differences in the activation energy of the oxidation of carbonaceous species derived from C_2H_4/He and C_2H_6/He reactions are shown to exist. Additional evidence related to the different kinds of carbonaceous species, which are derived from the C_2H_4 and C_2H_6 reactions with lattice oxygen species of Li^+-doped TiO_2, may be provided from the transient oxidation results shown in Fig. 3 (C_2H_4/He reaction) and the corresponding results reported earlier (C_2H_6/He reaction, Ref. (15)). In the case of C_2H_4/He reaction, the amount of carbonaceous species formed at 845°C is all reacted off the surface isothermally under oxygen treatment in the range 570–640°C. This transient isothermal oxidation produces only a single peak, likely suggesting the presence of a single kind of carbon species. On the other hand, in the case of C_2H_6/He reaction the amount of carbonaceous species reacted off the surface under oxygen treatment at a given temperature was found to strongly depend on temperature, and the shape of the CO_2 transients obtained suggests more than one kind of carbonaceous species (15).

Tables 5 and 6 illustrate, on a quantitative basis, large differences in the reactivity of lattice oxygen towards C_2H_6 and C_2H_4 as a function of Li^+-dopant concentration. This is obvious by comparison of the specific initial rates of reaction, R_1, as calculated from the transient responses (i.e., Fig. 1, spike at $t = 0$) at a given temperature. In the case of C_2H_6, the observed rates of CO_2 formation are larger by a factor of 5–10 over TiO_2 as compared to corresponding rates over Li^+-doped TiO_2 catalyst. This result could be attributed to the higher concentration of acidic sites present on the surface of TiO_2 as compared to Li^+-doped TiO_2, as previously reported (16), a factor that is expected to enhance cleavage of the C–C bond of the ethane molecule. The fact that in the case of C_2H_4 the effect of Li^+-dopant on the rate of reaction, R_1, is small (Table 6) is consistent with this scheme since it is more difficult to break the C═C bond in the C_2H_4 molecule than the C–C bond in the C_2H_6 molecule.

b. Reactivity of "Adsorbed" Oxygen Species towards C_2H_4 and C_2H_6

b.1. Effects of Li^+-dopant. The transient isothermal results of the reaction of C_2H_4 with the catalyst surface of TiO_2 in the absence (Fig. 6) and presence (Fig. 9b) of gas-phase oxygen clearly indicate large differences, both in the transient kinetics of each reaction and in the steady-state reaction rates obtained. The reaction rate values are summarized in Tables 5 and 6 for C_2H_6 and C_2H_4 over the undoped and Li^+-doped TiO_2 catalysts. It should be pointed out that gas-phase reactions between C_2-hydrocarbons and oxygen to form CO_2 over the temperature range investigated and under the experimental conditions employed were not present as stated under Results. Additional evidence for this is the decrease in the rate of CO_2 formation with increasing reaction temperature in the case of C_2H_4/O_2 reaction (Table 6). Therefore, the reaction rates calculated with C_2H_6/O_2 and C_2H_4/O_2 mixtures must reflect the influence of both "adsorbed" oxygen and lattice oxygen species on the oxidation reactions at hand.

In the case of C_2H_6, the results of Table 5 indicate that the initial rate of CO_2 formation due to reaction with lattice oxygen is greatly decreased in the presence of gas-phase oxygen for both undoped and Li^+-doped TiO_2 catalysts. However, in the case of C_2H_4 (Table 6) the rate of combustion of this molecule seems to be controlled by "adsorbed" rather than lattice oxygen species when gaseous oxygen is in the feed. These results could be explained based on the reactivity of "adsorbed" oxygen species towards total oxidation of C_2H_4 and C_2H_6 and the chemisorption characteristics of the hydrocarbon molecules on the catalyst surface. It is first noted that interaction of gas-phase oxygen with the surface of the present catalysts is likely to proceed according to Step [1] of the model presented above where various oxygen "adsorbed" intermediate species such as O^- and O_2^- might be formed, as has already been mentioned in a previous section. These "adsorbed" oxygen species have been reported to be stable with respect to gaseous O_2 (21). The presence of these "adsorbed" oxygen species increases the negative effective charge of the surface which might cause a decrease of the effective positive charge of surface Ti^{4+} and Li^+ cations. Considering the fact that C–C bond breaking may follow some kind of chemisorption step of C_2H_6 (i.e., via hydrogen bond with O^{n-} species (20)), it is conceivable that in the presence of gaseous O_2, activation of C_2H_6 into an appropriate transition chemisorbed state becomes a rate-limiting step, and subsequent oxidation steps, similar to those presented before (Steps [2]–[5]), are fast ones. Evidence for the latter is given in Tables 4 and 7, where it is shown that the activation energy for the oxidation (in the presence of gaseous O_2) of carbonaceous intermediate species formed after C_2H_6 reaction with the catalyst surface is smaller than that obtained based on the steady-state reaction rates of C_2H_6/O_2 with the catalyst surface.

It might be suggested that in the case of C_2H_6 reaction with the lattice oxygen of TiO_2 and Li^+-doped TiO_2 catalysts, the large decrease in the rate of oxidation obtained when gaseous oxygen is present in the feed could also be explained by evoking geometric restrictions on the chemisorption step of C_2H_6. Considering the regular arrangement of O^{2-} species on the TiO_2 surface and the fact that chemisorption of C_2H_6 may occur via a chemical bond between hydrogen atoms of the ethane molecule and O^{2-} species of the TiO_2 surface, it might be reasonable to suggest that "adsorbed" oxygen species sticking off the surface may hinder chemisorption of ethane.

In the case of C_2H_4, the results shown in Table 6 indicate that the initial rate of CO_2 formation due to reaction with the lattice oxygen is much smaller than that obtained in the presence of gas-phase oxygen, a result opposite to that found for C_2H_6, as discussed above. In addition, there is a decrease in the rate of CO_2 formation with increasing reaction temperature for the C_2H_4/O_2 reaction over Li^+-doped TiO_2, a result opposite to that obtained over the undoped TiO_2. Based on the previous discussion concerning the case of C_2H_6/O_2 reaction with respect to the effects of O^{n-} "adsorbed" species on the chemisorption of C_2H_6, one would expect similar effects for C_2H_4 as well. Interaction of C_2H_4 with "adsorbed" oxygen species on the surface would result in stronger chemisorption (stronger hydrogen bond with O^{n-} species) than in the case of C_2H_6. On the other hand, a possible interaction of the π-bond in the ethylene molecule with Ti^{4+} cations would result in a weaker bond in the presence of than in the absence of gaseous oxygen in the feed. Therefore, the increase in the rate of C_2H_4 oxidation to CO_2 due to the presence of "adsorbed" oxygen species (O^{n-}), as compared to that of C_2H_6, could be explained by an increase in the surface coverage of C_2H_4 as compared to that of C_2H_6. However, the observed increase in the rate of oxidation may not be justified only by an increase in the surface coverage of C_2H_4. It is suggested that the presence of "adsorbed" oxygen species may result in a lower activation energy for the rate-determining step(s) of the oxidation of intermediate CH_xO and/or CH_x species. The apparent activation energy value obtained from C_2H_4/O_2 reaction over TiO_2 (10 kcal/mol), as compared to that obtained from the oxidation of intermediate carbonaceous species formed after C_2H_4 reaction with lattice oxygen (23 kcal/mol), supports the explanation offerred above.

The decrease in the rate of C_2H_4 oxidation with increasing reaction temperature in the range 570–700°C over the Li^+-doped TiO_2 catalyst is considered to be due to the decrease in the surface coverage of adsorbed C_2H_4 intermediate species rather than to a change in the activation energy of the rate-limiting step(s) in the stated temperature range. An increase in the amount of surface carbon species which might block active sites with increasing reaction temperature is not likely, since O_2 titration experiments following reaction of C_2H_4/O_2 (Fig. 9) resulted in very small amounts of CO_2 at all reaction temperatures studied. These results are not obtained over the undoped TiO_2 catalyst (Table 6) and they clearly demonstrate the effect of Li$^+$-dopant on the interaction of C_2H_4 with the catalyst surface in the presence of gaseous oxygen.

b.2. Consequences of the reactivity of C_2H_4 and C_2H_6 with lattice and "adsorbed" oxygen species on the C_2H_4/ C_2H_6 product ratio obtained under OCM reaction conditions. The specific reaction rate results of C_2H_4 and C_2H_6 oxidation to CO_2 shown in Tables 5 and 6 might be used to explain the C_2H_4/C_2H_6 product ratio obtained over the present Li$^+$-doped TiO_2 catalyst under OCM reaction conditions, and also the relative contribution of C_2-hydrocarbons to the production of CO_2 under OCM reaction conditions. Before any discussion is made on these aspects, it must be made clear that the specific reaction rate results of C_2-hydrocarbon oxidation to CO_2 were obtained in the absence of CH_4 in the feed and, of course, are dependent on the C_2-hydrocarbon partial pressure. Concerning the first item, it is implied that the surface state of the catalyst studied may not be the same as that found under OCM reaction conditions (i.e., different coverage of adsorbed carbonaceous species which might influence the rate of C_2-hydrocarbons oxidation). Concerning the second item, a reaction order with respect to C_2-hydrocarbons and oxygen of unity is assumed.

We have previously reported kinetic results of the OCM reaction over the present 2 wt.% Li_2O-doped TiO_2 catalyst (16). At the reaction temperature 650°C, P_{CH_4} of 0.25 bar, and P_{O_2} of 0.05 bar, the intrinsic net rate of formation of C_2-hydrocarbons was found to be 18.8 μmol/min m^2, and the C_2H_4/C_2H_6 product ratio 0.1. Based on other experimental conditions used, the concentration of C_2 at the outlet of the reactor was found to be 0.91 mol.%. From the present results of C_2H_6/O_2 and C_2H_4/O_2 reactions at 650°C (see Tables 5 and 6), it is found that the rates of C_2H_6 and C_2H_4 consumption are 0.55 and 45.0 μmol/min m^2, respectively. These results can then be used to calculate the rate of consumption of C_2-hydrocarbons at the level of 0.91 mol.% and the other OCM reaction conditions previously mentioned. It is estimated that under these conditions the rate of C_2-hydrocarbon consumption due to surface oxidation to CO_2 is 0.43 μmol/min m^2. Therefore, the rate of C_2-hydrocarbon formation, without surface oxidation to CO_2, would be 19.2 μmol/min m^2, and the proportion of the rate of surface oxidation to the rate of formation of C_2-hydrocarbons would be 2.2%. Without considering possible effects of carbonaceous species present on the catalyst surface under OCM reaction conditions (13) on the rate of oxidation of C_2-hydrocarbons, it is rather clear from the above analysis that the decrease of the true rate of formation of C_2-hydrocarbons obtained under OCM reaction conditions over the present Li$^+$-doped TiO_2 catalyst, because of C_2-hydrocarbon combustion, must not exceed 5%.

Figure 11 presents the C_2H_4/C_2H_6 product ratio as a function of CH_4 conversion. The oxygen conversion is also shown as a function of CH_4 conversion in the Fig. 11. There is a rapid increase of the C_2H_4/C_2H_6 ratio at CH_4 conversions in the range 25–30%, which corresponds to 95–99% O_2 conversion. Thus, significantly more C_2H_4 than C_2H_6 is present in the reaction mixture when there is very little gas-phase oxygen in the reactor. This result is in harmony with the results shown in Tables 5 and 6 which show that the rate of C_2H_6 oxidation to CO_2 by lattice oxygen alone is much larger than that by "adsorbed" oxygen species, which are formed in the presence of gaseous O_2. In addition, the rate of C_2H_4 oxidation by lattice oxygen (in the absence of gaseous oxygen) is smaller than the rate of oxidation by "adsorbed" oxygen (in the presence of gaseous oxygen). Thus, at high oxygen conversions, ethane is oxidized much more rapidly than ethylene, giving rise to high C_2H_4/C_2H_6 ratios. However, as has been pointed out by one of the reviewers, dehydrogenation of C_2H_6 to C_2H_4 may be favoured on the present catalyst, at low gas-phase oxygen concentrations, giving rise to high C_2H_4/C_2H_6 ratios under these conditions. This explanation could also be appropriate for the results shown in Fig. 11.

b.3. Effects of catalyst pretreatment time in oxygen flow. The CO_2 transient results shown in Fig. 10 indicate

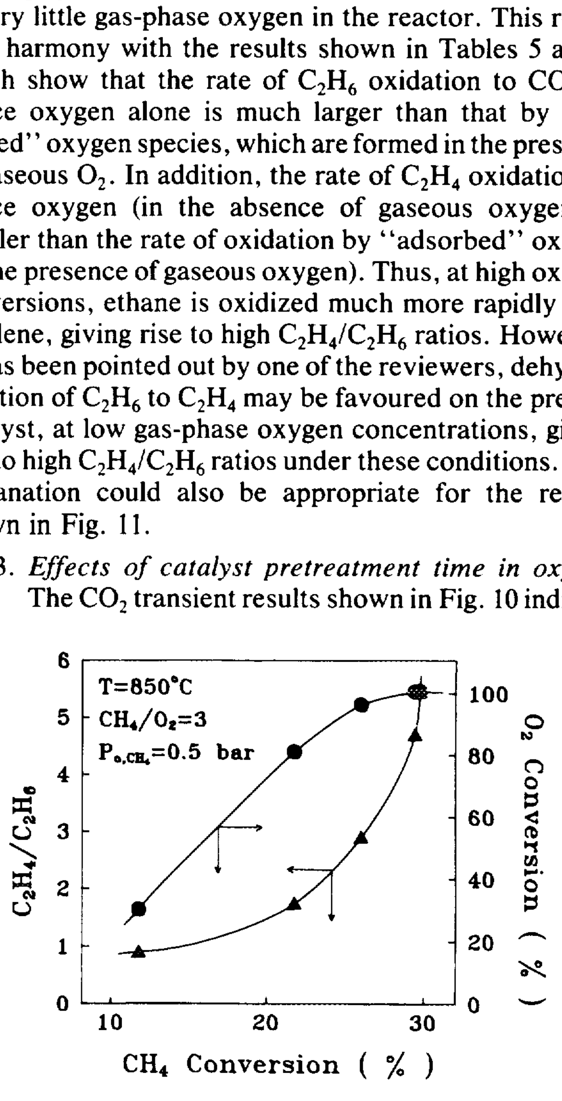

FIG. 11. Effect of CH_4 conversion on the C_2H_4/C_2H_6 product ratio obtained over 2 wt.% Li_2O-doped TiO_2 catalyst under OCM reaction conditions. T = 850°C, P_{CH_4} = 0.5 bar, CH_4/O_2 = 3. Also presented is the oxygen vs methane conversion relationship.

that upon passing the C_2H_6/O_2 mixture over the Li^+-doped TiO_2 catalyst at 820°C, there is an initial increase (overshoot) in the rate of CO_2 formation, followed by a very slow increase, and finally by a second overshoot much larger than the first one. The time of appearance of this second overshoot is a function of catalyst pretreatment time in O_2/He flow at 820°C. These results could be understood based on the kinetic model of oxidation of carbonaceous species presented under Results. It is first noted that following the second overshoot in the rate of CO_2 formation, a practically steady-state value in the rate is obtained, independent of oxygen pretreatment time (Fig. 10). During this steady-state condition the surface coverage of all intermediate species, particularly of those which are found in the reaction pathway, remains constant with reaction time. According to the kinetic model mentioned before, such species are, for instance, CH_x and/or CH_xO, adsorbed oxygen, oxygen vacancies, and hydroxyl groups. It is suggested that the oxygen pretreatment time influences the time of establishment of the steady-state coverages of the aforementioned species from their initial values upon passage of C_2H_6/O_2 over the catalyst surface.

Due to the long-term effects of oxygen pretreatment, it is reasonable to suggest that diffusion of Li^+ cations to the surface might be responsible for the results shown in Fig. 10. A small increase of Li^+ surface concentration under O_2 pretreatment could initially cause a decrease in the rate of oxidation of intermediate carbon species, while, after a few minutes, by the aid of gaseous oxygen, establishment of steady-state coverages of the various intermediate species occurs. This explanation is supported by the experimental evidence that over undoped TiO_2 the behaviour described in Fig. 10 has not been obtained, and also by the effects of Li^+-dopant on the C_2H_6/O_2 reaction as shown in Table 5. It seems unlikely that an oxygen pretreatment time of 2 h could have an effect on the kind of "adsorbed" oxygen species formed which might be responsible for the observed results. Transformation steps of "adsorbed," negatively charged oxygen species are generally considered as fast reaction steps (5).

c. *Kinetic Model for the Oxidation of Carbonaceous Species Formed after Reaction of C_2H_4 and C_2H_6 with Lattice Oxygen*

The mechanistic scheme proposed (Steps [1]–[6]) and the kinetics of the rate of oxidation of the intermediate species formed after reaction of C_2H_4 with the lattice oxygen of the undoped and Li^+-doped TiO_2 catalysts explain well the shift in the appearance of the maximum of the rate of CO_2 formation (Figs. 3 and 7) with temperature. Chemisorption of oxygen (Step [1]) was assumed to be a fast process. Evidence for that has been presented in a previous publication (17) using transient isotopic oxygen ($^{18}O_2$) exchange experiments. According to the present model, an increase in the maximum of the rate with increasing temperature should also be obtained (22), and this is indeed the case for the results shown in Figs. 3 and 7. On the other hand, in the case of C_2H_6 (Fig. 8) due to the oxidation of more than one kind of carbon species, this behaviour in the maximum of the rate is not pronounced for the temperature range 700–820°C, whereas in the case of Li^+-doped TiO_2 catalyst (15) an increase in the maximum of the rate with decreasing temperature has been observed. It is important to mention that the proposed kinetic model was checked by a second kind of experiment, that of temperature-programmed oxidation (Fig. 4), and the activation energy value obtained for the oxidation process is in good agreement with the value obtained from the isothermal oxidation experiments (Figs. 3 and 7). These results present some insight into the elementary steps of the oxidation process of CH_x and/or CH_xO species, which is found to be affected by the Li^+-dopant in the TiO_2 catalyst (compare E values in Table 4).

In the case of C_2H_6 reaction with the lattice oxygen of TiO_2, the isothermal oxidation experiments at various temperatures resulted in a different behaviour than that obtained with C_2H_4 (compare Figs. 7 and 8). In the case of C_2H_6, it is clear that more than one kind of carbonaceous species is formed after reaction with lattice oxygen at 700°C (Fig. 8) and, as in the case of C_2H_4, the Li^+-dopant causes an increase in the activation energy of oxidation of intermediate carbonaceous species (Table 4).

In the transient isothermal oxidation experiments presented in Figs. 3, 7, and 8, carbonaceous species have been deposited on the catalyst surface at 845°C. At this temperature, gas-phase disproportionation of C_2H_4 and C_2H_6, in the absence of gaseous oxygen, to form CH_x species may not be excluded. However, this temperature was chosen to be similar to that used under OCM reaction conditions. During this process of deposition of carbonaceous species, a nonuniform distribution may exist across the catalyst bed which could influence the observed shifts in the time of appearance of peak maxima with oxidation temperature. However, it should be stated here that Eq. [7] of the kinetic model is not a function of the initial coverage of carbonaceous species obtained before oxidation.

A recent steady-state tracing work of the OCM reaction over the present Li^+-doped TiO_2 catalyst (13), which had the objective of probing for the carbon pathway of CO_2 formation, and the present results of C_2-hydrocarbon reactivity with lattice and adsorbed oxygen species, suggest that it is difficult to evaluate rate constants of individual reaction steps (oxidation steps of carbonaceous species derived from CH_4 and C_2-hydrocarbons) using the only available $^{13}CO_2$ response curve (13). More precisely, it is not correct to evaluate a single rate constant, k, based on the relationship $k = TOF_{CO_2}/\theta_c$, where θ_c is the measured coverage of carbonaceous species which are found in the reaction pathway of CO_2 formation under OCM reaction conditions. Therefore, the present kinetic model and the activation energy values obtained (Table 4) for the oxidation pathway of carbonaceous species CH_x and/or CH_xO to form CO_2 are very useful.

d. Possible Rate-Limiting Steps of CO_2 Formation under OCM Reaction Conditions

The activation energy results shown in Table 7 could be used to discuss possible rate-limiting step(s) in the carbon pathway to form CO_2 under OCM reaction conditions. The apparent activation energy of CO_2 formation under OCM reaction conditions, as obtained in previous kinetic studies (16), was found to be 38 kcal/mol over the 2 wt.% Li_2O-doped TiO_2 catalyst. This value is similar to that obtained from the CH_4/He reaction (Table 7). It might be suggested that formation of carbon intermediate species derived from CH_4(CH_x, CH_xO) may control the overall rate of CO_2 formation under OCM reaction conditions.

In the case of undoped TiO_2, the activation energy results reported in Tables 4 and 7 may suggest that formation of carbonaceous species from C_2H_6 might be considered as one of the rate-limiting steps for the production of CO_2 under OCM reaction conditions. However, given the small fractional contribution of C_2-hydrocarbon oxidation (side reaction) to the overall rate of CO_2 formation under OCM conditions, the aforementioned step should not be considered as a rate-limiting step of the OCM carbon reaction pathway to form CO_2. In contrast, the possibility that formation and/or oxidation of carbonaceous species derived from CH_4 in the presence of gaseous oxygen being slow steps, may be considered.

CONCLUSIONS

The following conclusions are derived from the present work:

1. Lattice oxygen of Li^+-doped TiO_2 OCM catalyst is a total oxidation site for C_2H_4 and C_2H_6 in the temperature range 570–845°C. This site shows higher ability for C_2H_6 than C_2H_4 consumption to form gaseous CO_2 and carbonaceous species on the surface.

2. The kind and reactivity of carbonaceous species formed upon reaction of the lattice oxygen of Li^+-doped TiO_2 with C_2H_4 or C_2H_6 are different. However, oxidation of these carbonaceous species to CO_2 follows the same mechanism.

3. Adsorbed oxygen species formed by interaction of gaseous oxygen with the surface of Li^+-doped TiO_2 OCM catalyst appear to be much more reactive towards C_2H_4 than C_2H_6, a result opposite to that found for lattice oxygen.

4. Doping of TiO_2 with Li^+ cations results in a large decrease of lattice oxygen activity towards C_2H_6 and only in a small decrease towards C_2H_4 to form CO_2. However, an increase in the activity of adsorbed oxygen towards C_2H_4 and a decrease towards C_2H_6 to form CO_2 are observed.

5. Doping of TiO_2 with Li^+ cations affects the kinetics of oxidation of carbonaceous species formed upon reaction of C_2H_4 and C_2H_6 with the lattice oxygen. It is found that a stepwise dehydrogenation mechanism with at least two slow steps explains well the transient kinetics of this oxidation process.

6. The present results and others reported earlier (15, 16) suggest that formation of carbonaceous species from CH_4 might be considered as the rate-limiting step for the CO_2 production under OCM reaction conditions for the present Li^+-doped TiO_2 catalyst.

REFERENCES

1. Lunsford, J. H., *Catal. Today* **6,** 235 (1990).
2. Pitchai, R., and Klier, K., *Catal. Rev.—Sci. Eng.* **28,** 13 (1986).
3. Amenomiya, Y., Briss, V. I., Goledzinowski, M., Galuszka, J., and Sanger, A. R., *Catal. Rev.—Sci. Eng.* **32,** 163 (1990).
4. Wolf, E. E., Ed., "Methane Conversion by Oxidative Processes." Van Nostrand–Reinhold, New York, 1992.
5. Sokoloskii, V. D., *Catal. Rev.—Sci. Eng.* **32,** 1 (1990).
6. Dubois, J. L., and Cameron, C. J., *Appl. Catal.* **67,** 49 (1990).
7. Happel, J., "Isotopic Assessment of Heterogeneous Catalysis." Academic Press, San Diego, 1986.
8. Biloen, P., *J. Mol. Catal.* **21,** 17 (1983).
9. (a). Peil, K. P., Goodwin, J. G., and Marcelin, G., *J. Catal.* **131,** 143 (1991). (b). Peil, K. P., Goodwin, J. G., and Marcelin, G., *J. Catal.* **132,** 556 (1991).
10. Lacombe, S., Sanchez, J. G., Delichere, P., Mozzanega, H., Tatibouet, J. M., and Mirodatos, C., *Catal. Today* **13,** 273 (1992).
11. Kalenik, Z., and Wolf, E. E., *Catal. Today* **13,** 255 (1992).
12. Ekstrom, A., and Lapszewicz, J. A., *J. Am. Chem. Soc.* **110,** 5226 (1988).
13. Efstathiou, A. M., Lacombe, S., Mirodatos, C., and Verykios, X. E., *J. Catal.*, in press.
14. Ekstrom, A., and Lapszewicz, J. A., *J. Phys. Chem.* **93,** 5230 (1989).
15. Efstathiou, A. M., Papageorgiou, D., and Verykios, X. E., *J. Catal.* **141,** 612 (1993).
16. Efstathiou, A. M., Boudouvas, D., Vamvouka, N., and Verykios, X. E., *J. Catal.* **140,** 1 (1993).
17. Efstathiou, A. M., Papageorgiou, D., and Verykios, X. E., *J. Catal.* **144,** 352 (1993).
18. Papageorgiou, D., Efstathiou, A. M., and Verykios, X. E., *Appl. Catal.*, in press.
19. Bianchi, D., and Gass, J. L., *J. Catal.* **123,** 310 (1990).
20. Alka, K.-I., and Lunsford, J. H., *J. Phys. Chem.* **81**(14), 1393 (1977).
21. Gellings, P. J. and Bouwmeester, H. J. M., *Catal. Today* **12,** 1 (1992).
22. Bianchi, D., and Gass, J. L., *J. Catal.* **123,** 298 (1990).